HOKKAIDO UNIVERSITY

Title	Effects of phosphate ion concentration on in-vitro fibrillogenesis of sturgeon type I collagen
Author(s)	Meng, Dawei; Li, Wen; Ura, Kazuhiro et al.
Citation	International Journal of Biological Macromolecules, 148, 182-191 https://doi.org/10.1016/j.ijbiomac.2020.01.128
Issue Date	2020-04-01
Doc URL	https://hdl.handle.net/2115/80822
Rights	© 2020. This manuscript version is made available under the CC-BY-NC-ND 4.0 license https://creativecommons.org/licenses/by-nc-nd/4.0/
Rights(URL)	https://creativecommons.org/licenses/by-nc-nd/4.0/
Type	journal article
File Information	manuscript received 2020-06-09.pdf



Hokkaido University Collection of Scholarly and Academic Papers : HUSCAP

Effects of phosphate ion concentration on *in-vitro* fibrillogenesis of sturgeon type I collagen

Dawei Meng[a,b]*, Wen Li[b], Kazuhiro Ura[c], Yasuaki Takagi[c]

[a] *Zhejiang Province Joint Key Laboratory of Aquatic Products Processing, Institute of Seafood, Zhejiang Gongshang University, Hangzhou, China*

[b]*Graduate School of Fisheries Sciences, Hokkaido University, 3-1-1 Minato-cho, Hakodate, Hokkaido 041-8611, Japan*

[c]*Faculty of Fisheries Sciences, Hokkaido University, 3-1-1 Minato-cho, Hakodate, Hokkaido 041-8611, Japan*

E-mail addresses: mdw000@163.com (D. Meng), Kazu@fish.hokudai.ac.jp (K. Ura), takagi@fish.hokudai.ac.jp (Y. Takagi)

*Corresponding author

Tel./Fax: +86-19845265264, E-mail: dawei@mail.zjgsu.edu.cn (D. W. Meng)

Abstract

Nonmammalian collagens have attracted significant attention owing to their potential for use as a source of cell scaffolds for tissue engineering. Since the morphology of collagen fibrils controls cell proliferation and differentiation, its regulation is essential for fabricating scaffolds with desirable characteristics. In this study, we evaluated the effects of the phosphate ion (Pi) concentration on the characteristics of fibrils formed from swim bladder type I collagen (SBC) and skin type I collagen (SC) from the Bester sturgeon. An increase in the Pi concentration decreased the fibril formation rate, promoted the formation of thick fibrils, and increased the thermal stability of the fibrils for both SBC and SC. However, the SBC and SC fibrils exhibited different fibril formation rates, degrees of fibrillogenesis, morphologies, and denaturation temperatures for the same reaction conditions. Finally, by regulating the Pi concentration, various types of SBC and SC fibrils could be coated on cell culture wells, and fibroblasts could be cultured on them. The results showed that thin fibrils enhance fibroblast extension and proliferation, whereas thick fibrils restrain fibroblast extension but orient them in the same direction. The results of this study suggest that SBC fibrils, which exhibit diverse morphologies, are suitable for use as a novel scaffold material, whose characteristics can be tailored readily by varying the Pi concentration.

35 **Keywords:** Sturgeon type I collagen; Phosphate ion; Fibril formation; Fibril morphology;

36 Fibroblast morphology

37

1. Introduction

Type I collagen is the primary component of the extracellular matrix in skin, bone, and tendon [1]. Once its molecules have been secreted from cells, they spontaneously self-assemble into fibrils, which subsequently form thick fibers through a series of enzymatic and chemical reactions [2]. Collagen fibrils and fibers provide support for cell growth and ensure the mechanical resilience of connective tissues [3−4].

Under appropriate reaction-fluid conditions, extracted type I collagen molecules can form fibrils with structural, mechanical, and biological properties similar to those of native fibrils *in vivo* [5−7]. Because of their low antigenic activity, desirable cell adhesion properties, biocompatibility, and biodegradability, type I collagen fibrils have high potential for use as biomedical materials, such as cellular scaffolds for tissue engineering [8, 9]. When these fibrils are used as collagenous scaffolds, their morphological characteristics, including their diameter, shape, and orientation, have a determining effect on the adhesion, alignment, proliferation, and differentiation of anchorage-dependent cells [1, 10]. Therefore, the optimization of fibril morphology in scaffolds is essential for ensuring desirable cellular performance for various applications in tissue engineering.

Previous studies have shown that the ionic strength of the reaction fluid influences the *in-vitro* formation of collagen fibrils [11−13]. For example, Wood [14] found that the rate

of fibril formation and fibril width decrease with an increase in the ionic strength of the reaction fluid; the authors used NaCl to regulate the ionic strength. Divalent anions also play a critical role in regulating fibril formation rate [15]; in particular, phosphate ions are known to bind to collagen molecules, significantly affecting the electrostatic interactions between the molecules and, hence, the process of self-assembly of the collagen molecules into fibrils [15−17]. Because *in-vitro* collagen fibrillogenesis is a complex process affected by several factors, such as the electrostatic and hydrophobic interactions that occur as well as the intermolecular force involved [16, 18], the mechanism through which the ionic strength affects collagen fibrillogenesis remains unknown. Therefore, a better understanding of the effects of the ionic strength on the fibril morphology will allow for the rational design of collagen-based scaffolds.

Currently, the most common collagen sources for biomedical use are bovine skin and tendon, porcine skin, and rat tail [19−21]. However, animal collagen-containing products can potentially include components that cause infectious animal diseases in humans, including bovine spongiform encephalopathy, foot-and-mouth disease, and African swine fever [22]. Religious beliefs also restrict the use of some animal products [23]. Therefore, alternative collagens extracted from marine sources, especially from fish byproducts, such as skin, scales, and bones, attracted increasing attention [20, 21, 24−26]. Our recent research has shown that

74 mammalian and fish collagen have different biochemical and physicochemical characteristics,
75 including different amino acid compositions, thermal stabilities, and fibril-forming abilities
76 [27]. Therefore, to take advantage of marine collagens as biomedical materials, it is necessary
77 to elucidate their characteristics, especially their fibril-forming ability and the factors that
78 determine the morphological characteristics of the fibrils formed *in vitro*. Compared to the
79 case of mammalian collagens, however, there is limited knowledge regarding marine
80 collagens and their fibrillogenesis properties.

81 In a previous study [27], we showed that the sturgeon contains a large amount of type
82 I collagen in its byproducts, including its swim bladder and skin. The pepsin-treated collagen
83 (atelocollagen) from these tissues reassembled into fibrils more quickly than mammalian
84 collagen under specific conditions, suggesting that the former may be suitable for fabricating
85 biomedical materials [27]. We also found that increasing the ionic strength of the reaction
86 solution by adding NaCl sped up the fibrillogenesis process and promoted the formation of
87 thicker fibrils. Notably, the swim bladder collagen assembled into a unique fusiform structure.
88 These findings suggest that sturgeon collagens can potentially be used to form fibrils of
89 different morphologies by controlling the reaction-fluid environment.

90 The objective of the present research is to clarify the regulation ability of the fibril
91 morphology of sturgeon collagens to evaluate their potential as scaffold materials for tissue

92 engineering. Specifically, we elucidated the effects of the phosphate ion (Pi) concentration of
93 the reaction fluid on the *in-vitro* formation of fibrils of swim bladder type I collagen (SBC)
94 and skin type I collagen (SC). Other ion species, including cations, and the pH of the reaction
95 fluid may also affect the electrostatic interactions between the collagen molecules and, hence,
96 their self-assembly to fibrils. However, Pi is the first choice, since it has been proven to bind
97 to collagen molecules and regulate fibril formation [28]. As a first step, we evaluated the
98 effects of Pi concentration on the fibrillogenesis of SBC and SC because, to date, there has
99 not been any research on the influences of Pi on the fibrillogenesis of fish collagen. Based on
100 our findings, we successfully coated different forms of SBC and SC fibrils on cell culture
101 wells by regulating the Pi concentration of the reaction fluid and evaluated the proliferation of
102 fibroblasts on them along with the morphology of the fibroblasts.
103
104 **2. Materials and methods**
105 2.1. Isolation and purification of collagen
106 A Bester sturgeon (*Huso huso* × *Acipenser ruthenus*; body weight of 6.0 kg) was
107 procured from the Nanae Fresh-Water Laboratory, Field Science Center for Northern
108 Biosphere, Hokkaido University, Japan. Its swim bladder and skin were dissected, washed
109 with chilled tap water, lyophilized, and stored at -30 °C until use. Before the collagen

110 extraction process, the skin fat was removed during a period of 24 h using 99.5% ethanol (two
111 solution changes) in a sample/solution ratio of 1/10 (w/v). Then, the swim bladder and
112 defatted skin were cut into small pieces (ca. 0.5 × 0.5 cm) for collagen extraction. Extraction,
113 purification, and freeze-drying were performed as per the procedures reported by Meng et al.
114 [29].
115
116 2.2. *In-vitro* collagen fibrillogenesis
117 Collagen fibrillogenesis was performed according to the method of Meng et al [29],
118 with modifications of the Na-phosphate buffer (PB) concentrations. Freeze-dried SBC and SC
119 were dissolved in a HCl solution (pH 2.0) at a concentration of 0.3% (w/v). Subsequently,
120 these SBC and SC solutions were mixed with a Na-phosphate buffer (pH 7.4) solution, having
121 a Na-phosphate concentration of 22.5, 45, 90, or 180 mM, respectively; the collagen
122 solution/PB ratio was set to 1/2 (v/v), which resulted in a final PB concentration of 15, 30, 60,
123 or 120 mM, respectively. The mixtures were kept at 21 °C, and fibril formation was
124 monitored during a period of 1 h in terms of the changes in turbidity based on the absorbance
125 at 320 nm; this was done using a spectral monitor (Hitachi High-Technologies Corporation,
126 Tokyo, Japan).
127

2.3. Degree of collagen fibrillogenesis

The degree of collagen fibrillogenesis was measured using the method proposed by Zhang et al. [27]. In brief, the reacted solution was centrifuged at 20,000×*g* for 20 min to precipitate the fibrils, and the protein content of the supernatant was measured based on the method reported by Lowry [30]; bovine serum albumin was used as the standard. The degree of collagen fibrillogenesis was defined as the percentage of decrease in the collagen concentration. In other words, it was defined as the percentage of collagen molecules that formed fibrils.

2.4. Morphology of fibrils formed

The microstructures of the SC and SBC fibrils were observed using a scanning electron microscopy (SEM) system (JSM6010LA, JEOL Ltd., Tokyo, Japan). The collagen fibrils were formed as described in Section 2.2 and obtained by centrifugation as described in Section 2.3. The precipitated fibrils were fixed with 2.5% (v/v) glutaraldehyde in 0.1 M PB (pH 7.4) for 3 h at room temperature, rinsed with PB to remove the fixative, dehydrated using a graded series of ethanol solutions, and soaked in a t-butyl alcohol solution for two 30-min intervals. Finally, the samples were freeze-dried in a t-butyl alcohol solution using a freeze-drying device (JFD-320; JEOL Ltd.) and coated with gold-platinum, using an auto fine

146 coater (JFC-1600; JEOL Ltd.). After the SEM observations, digital images of the samples
147 were taken, and the diameters of 100 randomly selected fibrils were determined using the
148 software ImageJ. The measurements were performed three times using different photographs.
149
150 2.5. Thermal stability of collagen fibrils
151 The maximum transition temperatures (T_m) of the reassembled fibrils of SBC and SC
152 were measured by differential scanning calorimetry (DSC; EXSTAR DSC6100, SII Nano
153 Technology Inc., Chiba, Japan). The collagen fibrils were prepared as described in Section 2.4,
154 placed in an aluminum pan (70 μl), and DSC measurements were performed from 20 to 70 °C
155 at a rate of 3 °C/min. An empty aluminum pan was used as reference. The T_m value was taken
156 to be the temperature corresponding to the endothermic peak in the DSC curve.
157
158 2.6. Coating of collagen fibrils on cell culture wells
159 A 200 μl aliquot of a 1% (w/v) SBC or SC solution (pH 2.0) was placed in each cell
160 culture well (24-well cell culture plate; FALCON, Durham, NC) and kept there for 30 min.
161 Then, the solution in each well was replaced with 200 μl of PB (15, 30, 60, or 120 mM; pH
162 7.4), and fibril formation was induced for 1 h. After removing the PB solution, a PB solution
163 with the same Na-phosphate concentration but containing 0.1 mM genipin as a crosslinker

was added, and the wells were stored for 12 h. Finally, the genipin-PB solution was removed, and the wells were washed twice with Hanks balanced salt solution , containing 100 U/ml penicillin and 100 μg/ml streptomycin, and immediately used for cell culture experiments. A diluted HCl solution (pH 2.0) was used instead of the SBC or SC solution as the control. All procedures were performed under aseptic conditions at 21 °C.

2.7. Morphology of collagen fibrils formed on cell culture wells

After the formation of the collagen-fibril coating, the bottom surface of each well was fixed, dehydrated, and freeze-dried by removing the solutions as described in Section 2.4. After the completion of the freeze-drying process, the bottom of each well was removed and cut into a 1×1 cm piece using a heated scalpel. The surface was coated with gold-platinum and observed using SEM.

2.8. Cell culturing

To study the cell morphology and proliferation on the SBC and SC collagen fibrils, we used L929 mouse fibroblastic cells maintained in Eagles minimum essential medium (Life Technologies Corporation, Grand Island, NY, USA) supplemented with a 5% fetal bovine serum (Thermo Fisher Scientific, Carlsbad, CA, USA) and a 1% penicillin/streptomycin

182 mixture (Thermo Fisher Scientific, Grand Island, NY, USA). The cells were cultured for 5
183 days in a humidified incubator at 37 °C and 5% CO_2; the medium was renewed after 3 days.
184
185 2.9. Cell morphology and proliferation
186 The morphology of the cells was observed over the cell-culture period using a
187 phase-contrast microscope (DMI600B, Leica, Wetzlar, Germany). The microstructure of the
188 cells 2 days after seeding was observed by SEM as described in Section 2.7.
189 A cell counting kit (CCK-8, DOJIN, Mashiki, Japan) was used to evaluate the
190 cell-proliferation activity. After a 5-day culture, the culture medium was removed, and the
191 culture was washed with PBS twice. Then, 540 μl of the culture medium and 60 μl of the
192 CCK-8 solution were added to each well, and the cells were cultured for 30 min. The
193 supernatant (100 μl) was transferred to a 96-well plate, and the optical density at 450 nm was
194 determined using a microplate reader (infiniteF50R, Wako, Osaka, Japan). Six parallel
195 replicates were read for each sample.
196
197 2.10. Statistical analysis
198 The data on the degree of fibril formation and the proliferation of L929 cells are
199 expressed as mean ± standard error. Significance was set to $p < 0.01$. The data were analyzed

200 using ANOVA and Tukey–Kramer post-hoc tests for multiple comparisons, which were
201 performed using a statistical add-in for Microsoft Excel (SSRI, Tokyo, Japan).
202
203 **3. Results**
204 3.1. Collagen fibrillogenesis
205 The effects of the Pi concentration on the progression of SBC and SC fibril formation
206 *in vitro* are shown in Fig. 1. When the Pi concentrations of the PB solution were 15 and 30
207 mM, the initial turbidity in the case of SBC was higher than 0.5 and increased sharply without
208 a lag phase. As the Pi concentration increased to 60 mM, however, a short lag phase appeared
209 before the growth phase. At a Pi concentration of 120 mM, the turbidity curve was sigmoidal
210 and contained an extended lag phase and a more gradual growth phase. The turbidity in the
211 plateau phase was also affected by the Pi concentration: it was highest at 60 mM, followed by
212 the turbidity at 120, 30, and 15 mM. The same trend was observed in the turbidity curves for
213 SC. However, no increase in the turbidity was observed at a Pi concentration of 120 mM. In
214 addition, for SC and a Pi concentration of 60 mM, the turbidity in the plateau phase was lower
215 than that for SBC.
216
217 3.2. Degree of fibrillogenesis

The degree of fibrillogenesis was assessed after 1 h (Fig. 2). For both SBC and SC, the degree was higher than 95% when the Pi concentration was less than 30 mM. Further, it decreased to 89% for SBC and 60% for SC when the Pi concentration increased to 60 mM. At a concentration of 120 mM, the fibrillogenesis degree decreased to 64% in SBC, while no collagen fibrils were formed in SC, which conformed with the SC turbidity curve.

3.3. Morphology of fibrils

SEM images of the SBC and SC fibrils formed after incubation for 1 h are shown in Fig. 3, while the diameter distributions of the fibrils are shown in Fig. 4. Hereafter, the fibrils are referred to on the basis of the origin of the collagen used (swim bladder or skin) and the Pi concentration at the time of fibrillogenesis (15−120 mM). Hence, SBC-15 refers to the fibrils formed using SBC and a Pi concentration of 15 mM. At the lowest phosphate concentration (15 mM), thin fibrils curled together in high density were formed in both SBC and SC (Fig. 3). The mean diameters were 77.7 nm for SBC-15 and 78.8 nm for SC-15, and the fibril diameter distributions were narrow (Fig. 4). As the Pi concentration increased, thicker fibrils appeared for both SBC and SC (Fig. 3). As a result, the range of the fibril diameters also increased (Fig. 4). The largest mean diameters were observed in the cases of SBC-60 (397 nm) and SC-60 (238 nm). In addition, the SBC-30 preparation included thick but short fusiform structures

(Fig. 3). At a Pi concentration of 60 mM, the fusiform structures became larger and were characterized by a transverse periodic banding pattern (Fig. 3). These fusiform structures were interlaced with thin fibrils, with a maximum diameter of more than 1600 nm (Fig. 4). In SBC-120, the fusiform structures disappeared. However, the mean fibril diameter was higher than that of SBC-60 (Figs. 3 and 4). In the SC fibrils, no fusiform structures were observed, but thick fibril bundles were present in SC-30 (Fig. 3). In contrast to the case for the fusiform structures in SBC, these bundles were probably formed by the spiral assembly of the thin fibrils (Fig. 3). Finally, these bundles were not present in SC-60. However, the diameter of the fibrils was higher than that of the fibrils in SC-30 (Figs. 3 and 4).

3.4. Thermal stability of collagen fibrils

The DSC curves of the SBC and SC fibrils are shown in Fig. 5. The T_m value of the SBC fibrils increased as the Pi concentration increased to 60 mM but decreased once the Pi concentration was 120 mM. The values for SBC-15, SBC-30, SBC-60, and SBC-120 were 42.9, 43.3, 44.1, and 40.4 °C, respectively. Further, for the same Pi concentration, the T_m values of the SC fibrils were lower than those of the SBC fibrils, with the values of SC-15, SC-30, and SC-60 being 37.7, 40.7, and 44.7 °C, respectively.

3.5. Collagen-fibril coating on cell culture wells

In this study, a two-dimensional collagen-fibril coating was formed in cell culture wells to study the cell growth and proliferation characteristics of the different collagen fibrils. SEM images of the SBC- and SC-fibril coatings are shown in Fig. 6. Both the SBC and SC fibrils were aligned along the same direction on the bottoms of the culture wells. Although the trend in the Pi-dependent changes in the fibril diameter was the same as that for the fibrils formed in solution, the fibrils coated on the wells were thinner. In addition, the SBC fibrils exhibited greater variation in their diameter with changes in the Pi concentration of the buffer. The fusiform structures were observed only in SBC-60. Finally, the bundle structures were not observed in the SC fibrils.

3.6. Cell morphology

Figure 7 shows the morphologies of the L929 cells grown on the SBC and SC fibrils. Six hours after seeding, the cells on all the fibrils were highly stretched, except for those on the SBC-60 and -120 fibrils. In the cases of the SBC-60 and SBC-120 fibrils, the cells were attached firmly but were round and did not spread. Twenty-four hours after seeding, the number of cells increased. This was true for all the cases. Further, the cells spread randomly on the control surface and the fibrils, apart from those in the SBC-60 and -120 samples. On

the SBC-60 and -120 fibrils, in contrast, cells began to spread in the same direction, parallel to the fibrils.

To further examine cell morphology, the cells were imaged using SEM 2 days after seeding (Fig. 8). The cells on the control surface were flat and irregular. In contrast, the cells on both the SBC and SC fibrils had a higher cell height (thickness). Furthermore, many of the cells exhibited two long protrusions into the counter direction. All the cells on the SC fibrils were stretched far more than those on the SBC fibrils and irregularly oriented. Similarly, the cells on the SBC-15 and -30 fibrils were also misaligned, while those on the SBC-60 and -120 fibrils displayed a higher degree of alignment along the fibril direction.

3.7. Cell proliferation

Cell proliferation was assessed on day 5, using a CCK-8 kit (Fig. 9). The cells on the fibril-coated wells proliferated at a significantly lower rate than those on the control wells. The cells on the SC fibrils showed a higher proliferation activity than those on the SBC fibrils. Moreover, no significant differences were observed between the SC-15, -30, and -60 groups. Cell proliferation on the SBC fibrils decreased with an increase in the Pi concentration from 15 to 60 mM and was lowest on the SBC-60 fibrils and highest on the SBC-120 fibrils.

4. Discussion

The results obtained in this study clearly showed that the Pi concentration in the reaction fluid significantly affects the rate of *in-vitro* fibril formation as well as the morphology of the fibrils formed. This inference is true for both SBC and SC. There have been a few studies on the fibrillogenesis of type I collagen and the morphology of the fibrils formed *in vitro* in fish collagens, such as those from salmon skin [26], shark skin [31], red stingray skin [32], Bester sturgeon skin, and swim bladder [27]. However, these studies focused on the influence of monovalent ions only, such as Na^+ and Cl^-. Because divalent anions have a higher order in the Hofmeister series, they have a greater effect on macromolecules and larger ions [33]. A few studies on fibrillogenesis in mammalian collagens found that divalent anions have a more pronounced effect than monovalent anions [15, 34]. To the best of our knowledge, the present study is the first to elucidate the effects of the Pi concentration on the fibrillogenesis process and the morphology of the fibrils formed *in vitro* in fish collagens. As known from previous studies, ionic strength also affects collagen fibrillogenesis [11−14]. Therefore, Pi concentration and ionic strength may work together to change collagen fibrillogenesis in the present study.

Collagen fibrillogenesis is a complex process of molecular assembly, which can be studied based on the changes in turbidity corresponding to three phases: a lag phase, wherein

there is no change in the turbidity; a growth phase, which involves a rapid increase in the turbidity; and a plateau phase, during which the turbidity again remains unchanged. Ultrastructural studies on fibrillogenesis using atomic force microscopy have revealed that the lag and growth phases consist of several multistep processes [35, 36]. During the lag phase, multiple coassemblies of several collagen molecules (nucleation) form and their nuclei subsequently undergo linear aggregation to produce subfibrillar units [37]. Then, these subfibrillar units aggregate laterally to form fibrils, which then grow into bundles during the growth phase [38]. Silver et al. [39] reported that fibril formation occurs at the end of the lag phase and that only the mass of the fibrils increases during the growth phase. The subfibrillar units have a determining effect on the mechanical properties of collagen fibers [37].

In this study, the addition of Pi significantly prolonged the lag phase of the fibrillogenesis process in both SBC and SC. At Pi concentrations of 15 and 30 mM, the initial turbidities were higher than those at 60 and 120 mM; this was true for both SBC and SC, suggesting that the lag phase was shorter than the time taken for the first absorbance measurement (less than 5 s after the mixing of the collagen solution and PB). As the Pi concentration increased, the lag phase became longer. Previous studies on mammalian collagens have indicated that phosphate ions direct the linear and lateral growth of collagen molecules [15, 38, 39]. Therefore, we can conclude that one of the primary effects of the Pi

326 concentration on fibril formation in SBC and SC is related to subfibrillar unit formation
327 during the lag phase. A shorter lag phase was observed at lower Pi concentrations, suggesting
328 that the nucleation and linear aggregation of the nuclei into subfibrillar units was accelerated
329 in these cases. Under such conditions, numerous small subfibrillar units may form within a
330 short period. As the Pi concentration increased, the lag phase became longer, and a few larger
331 subfibrillar units were produced slowly. Hayashi [15] reported that the lag phase during
332 polymerization is a unique feature of the assembly mechanism. Hence, the Pi concentration
333 probably has a determining effect on these molecular interactions of collagen.
334 Collagen fibril formation is a complex process operating under many secondary
335 forces, such as electrostatic interaction, hydrogen bonding, or salt bridging. Some studies on
336 mammalian collagens suggested that the Pi concentration has a significant effect on the
337 electrostatic interactions that occur between collagen molecules [15−17] and that the
338 assembly of subfibrillar units is primarily controlled by these electrostatic interactions [15].
339 For example, Li et al. [16] found a strong influence of Pi on the surface charge of collagen
340 molecules, which would change the electrostatic repulsion and regulate the aggregation of
341 such molecules. This process mainly occurred in the lag phase. Thus, the Pi concentration
342 probably affects the lag phase during SBC and SC fibril formation through electrostatic
343 interactions occurring between SC and SBC molecules, respectively.

The growth phase involves the lateral aggregation of the subfibrillar units to form higher-molecular-weight fibrils. The slope of the turbidity curve reflects the rate of lateral aggregation, while the final turbidity is reflective of the fibril diameter [11]. Zhu and Kaufman [40] reported that the increase in turbidity during the growth phase is primarily attributable to an increase in the fibril diameter. In the present study, as the Pi concentration increased, the slope corresponding to the growth phase decreased, and the turbidity was high. These results suggest that the larger subfibrillar units that are formed at higher Pi concentrations require more time to aggregate and form thicker fibrils. The results of the SEM observations of the fibrils supported this hypothesis, namely, that a higher Pi concentration in the growth environment induces the formation of thicker fibrils with an elongated morphology. This tendency was observed in both SBC and SC but more evident in the former. As was also the case in the present study, Hayashi et al. [15] examined fibril formation in calf skin collagen for Pi concentrations of 50–300 mM and found that the fibril formation rate decreased with an increase in the Pi concentration. Further, Williams et al. [41] reported that Pi concentrations lower than 30 mM had negligible effect on the fibril formation rate in rat tendon collagen. In contrast, the formation rate decreased for Pi concentrations higher than 30 mM. However, few studies have directly described the relationship between fibril morphology and Pi concentration.

362 Different types of thick fibril-based structures were formed in SBC and SC at various
363 Pi concentrations. Fusiform fibril structures grew in SBC at Pi concentrations of 30 mM and
364 60 mM. In contrast, thick bundles of fibrils formed in SC at a Pi concentration of 30 mM.
365 These results indicated that the processes of fibril formation were different in the type I
366 collagens obtained from the swim bladder and skin of the sturgeon. In a previous study, we
367 found that the hydroxyproline (Hyp) content of SBC is higher than that of SC [27]. Since the
368 hydroxyl groups of Hyp form hydrogen bonds to maintain the structure and stability of
369 collagen, the difference in the Hyp contents of SBC and SC may be one of the reasons for
370 different structures forming in the two types of collagens. This difference in the Hyp contents
371 of SBC and SC may be attributable to a difference in the composition of the α-chains in the
372 collagen molecules, as is characteristic in fish. The molecules of type I collagen from
373 mammals form a triple helical heterotrimer with two identical α1(I) chains and one α2(I)
374 chain and can be expressed as $[\alpha1(I)]_2\alpha2(I)$. Although minor collagen molecules, including
375 those of type V, are usually found with type I collagen, the composition of the type-I α chain
376 in different tissues is the same. In the molecules of the type I collagen found in fish, however,
377 another type of α-chain, named α3(I), is present [42]. Therefore, the type I collagen molecules
378 in fish are a mixture of $[\alpha1(I)]_2\alpha2(I)$ and α1(I)α2(I)α3(I), with the ratio of the two types of
379 molecules being specific to each tissue. Zhang [43] reported that the mRNA expression levels

of the α1(I) and α2(I) chains in the swim bladder and skin of the Amur sturgeon are different. Thus, a difference in the ratios of α1(I), α2(I), and α3(I) of SBC and SC could be the primary reason for the difference in the Hyp contents.

The diameter ranges of the fibrils formed during the *in-vitro* fibrillogenesis experiments in SBC and SC were 50–1600 nm and 50–350 nm, respectively. The thicknesses of collagen fibrils *in vivo* are 0.5–3 μm [44, 45]. This suggests that, at the right Pi concentration, sturgeon collagen can form fibrils with diameters similar to those of the fibrils formed *in vivo*. Hence, sturgeon collagen can potentially be used as a biomedical material. In addition, the T_m value of the fibrils increased with the Pi concentration. In one of our previous studies, we found that the concentration of NaCl showed no effect on the thermal stability of the fibrils [46]. This indicates that the effects of phosphate ions on collagen fibrils are different from those of NaCl. The precise mechanism responsible for this increase in T_m remains to be clarified. However, it is likely that the structural differences between the fibrils are responsible for the observed T_m values.

The present study also showed that higher Pi concentrations inhibit the number of fibrils formed over a period of 1 h (Fig. 2). This effect was more pronounced in SC than in SBC, with no SC fibrils forming at a concentration of 120 mM. It is possible that, as the Pi concentration increased, more collagen molecules undergo linear aggregation to form large

398 subfibrillar units, owing to a decrease in the degree of lateral aggregation. The subfibrillar
399 units were probably too narrow to affect the turbidity and could not be collected by
400 centrifugation. Currently, performing *in-situ* observations of the developing subfibrillar units
401 remains a challenge because a technique with a molecular-level resolution is required. The
402 development of such techniques will improve our understanding of the mechanisms by which
403 the Pi concentration affects fibril morphology.

404 We further attempted to use the SBC and SC fibrils as cellular scaffolds for tissue
405 engineering, since collagen fibrils are the primary scaffolds *in vivo*. Therefore, we coated
406 SBC and SC fibrils on cell culture wells and examined the responses of fibroblastic L929
407 cells in terms of their morphology and proliferation. The L929 cells seeded on the control
408 wells had irregular polygonal shapes and proliferated rapidly in a tilted manner on the bottom
409 surfaces of the wells. In contrast, the cells seeded on the collagen fibrils had higher cell height
410 (larger cell thickness), and many of them extended two long cellular processes in the opposite
411 direction. Notably, the cells attached to the SBC-60 and -120 fibrils spread the cellular
412 processes along the fibrils.

413 This type of cell morphology can be attributed to the specific signal transduction
414 from the fibrils, which passed through the integrins and transformed the cellular receptors to
415 type I collagen fibrils [47]. Generally, the signaling pathways downstream of the integrins

416 regulate different aspects of cell behavior, such as cell morphology, orientation, proliferation,
417 and differentiation [48−50]. According to Friedrichs et al. [44], cells expressing integrins are
418 polarized strongly along collagen fibrils. In contrast, cells lacking integrins attach to the
419 substrates but do not exhibit polarization.

420 We were also able to determine the appropriate fibril diameter range for cell
421 polarization. Because the cells in some human tissues, such as bone and tendon, are arranged
422 in parallel arrays [51], being able to regulate the cell direction is essential for tissue
423 engineering. Thus, the SBC-60 and -120 fibrils have high potential for use as scaffolds for the
424 engineering of tissues consisting of aligned cell arrays.

425 The cell proliferation rate on the SBC and SC fibrils was lower compared to that on
426 the control (noncoated) surface. On the SBC fibrils, effects of fibril diameter on the
427 proliferation activity were apparent: as the fibril diameter increased, the cell proliferation
428 activity decreased, with the activity being lowest at a Pi concentration of 60 mM. Thus, the
429 cells probably receive different signals for proliferation from fibrils having different diameters.
430 Artavanis-Tsakonas [52] found that signal transmission between cells also affects cell
431 proliferation. Thus, it is possible that the high degree of cell alignment on the SBC-60 and
432 -120 fibrils causes the transmission of different signals, resulting in a decrease in proliferation.
433 Mouse MC3T3E1, ATDC5, 3T3-L1, and C2C12 cells also exhibit reduced proliferation on

SBC fibrils, especially when the fibril diameter is high [53]. While the exact reason for this phenomenon is yet unknown, it suggests that the inhibitory activity of SBC fibrils is not specific to L929 cells. This study has a limitation in that the effects of SBC fibrils on cellular differentiation were not determined. Since there is a general trade-off relationship between cell proliferation and differentiation, SBC fibrils may also affect the latter. Future studies on the differentiation of cells on SBC fibrils will further clarify the potential of SBC fibrils as cellular scaffolds. In addition, the present method is not applicable to the standard three-dimensional cell culture system containing cells in the collagen gel. Since the standard method seeds the cells in a mixture of collagen and the cell culture medium and, thereafter, induces gelation, the high Pi concentrations used for the regulation of collagen fibrillogenesis in this study may have had some adverse effects on the cells. Future studies on the application of the present method to the three-dimensional scaffold and cell culturing are essential.

5. Conclusions

In this study, the regulation ability of the fibril morphology of sturgeon collagens was clarified to demonstrate their potential as scaffold materials for tissue engineering. It was found that the Pi concentration has a determining effect on the morphology as well as the rate and degree of fibrillogenesis and the thermal stability of the formed fibrils. At low Pi

concentrations, thin fibrils with a low thermal stability were formed. However, as the Pi concentration increased, the fibril formation rate decreased, and thick fibrils with higher thermal stability were formed. Moreover, the morphology of the fibrils determined the morphology and proliferation of the fibroblasts grown on them. We could successfully coat SBC and SC fibrils of different morphologies on the bottoms of cell culture wells and found that, while thin fibrils are better for cell extension and proliferation, thick fibrils limit cell extension and proliferation but regulate cell orientation. Given that there have been no previous studies on the effects of Pi concentration on the characteristics of fish collagen fibrils, this study is the first to highlight the possibility of Pi-induced regulation of the morphology of sturgeon collagen fibrils from a tissue engineering viewpoint. In particular, SBC is suitable for use as a scaffold material, because SBC fibrils are rich in sturgeon by-products [27], quicker to assemble [27, 29], retain high Tm (higher than 37 °C), are affected by the Pi concentration to a greater degree, and exhibit a more diverse morphology as compared to SC fibrils. Future studies on the differentiation of cells on SBC fibrils will further clarify the potential of SBC fibrils as cellular scaffolds.

Acknowledgments

This study was partly supported by the Grant-in-Aid for Challenging Research (Exploratory) (19K22322), MEXT, Japan. We would like to thank Editage (www.editage.jp) for English language editing. We also thank Takayuki Miura, Hiroki Kotake, Syoichi Moroi, and Takashi Tamura for their assistance with the cell culture experiments.

References

[1] J. A. Vranka, E. Pokidysheva, L. Hayashi, K. Zientek, K. Mizuno, Y. Ishikawa, K. Maddox, S. Tufa, D. R. Keene, R. Klein, H. P. Bachinger, Prolyl 3-hydroxylase 1 null mice display abnormalities in fibrillar collagen-rich tissues such as tendons, skin, and bones, *J. Biol. Chem.* **285**, 2010, 17253−17262.

[2] A. G. Galicka, Mutations in type I collagen genes resulting in osteogenesis imperfecta in humans, *Acta. Biochim. Pol*. **49**, 2002, 433−441.

[3] K. Wolf, S. Alexander, V. Schachtc, L. M. Coussens, U. H. von Andriane, J. Rheenen, E. Deryugina, P. Friedl, Collagen-based cell migration models in vitro and in vivo, *Semin. Cell. Dev. Biol.* **20**, 2009, 931−941.

[4] S. S. Sivan, A. J. Hayes, E. Wachtel, B. Caterson, Y. Merkher, A. Maroudas, S. Brown, S. Roberts, Biochemical composition and turnover of the extracellular matrix of the normal and degenerate intervertebral disc, *Eur Spine J*. **23**, 2014, S344−S353.

[5] F. H. Silver, J. W. Freeman, G. P. Seehra, Collagen self-assembly and the development of tendon mechanical properties, *J. Biomech*. **36**, 2003, 1529−1553.

[6] L. E. R. O`Leary, J. A. Fallas, E. L. Bakota, M, K. Kang, J. D. Hartgerink, Multi hierarchical self-assembly of a collagen mimetic peptide from triple helix to nanofiber and hydrogel, *Nat. Chem*. **3**, 2011, 821−828.

491 [7] R. A. MacDonald, B. F. Laurenzi, G. Viswanathan, P. M. Ajayan, J. P. Stegemann,
492 Collagen–carbon nanotube composite materials as scaffolds in tissue engineering, *J. Biomed.*
493 *Mater. Res*. **74**, 2005, 489−496.
494 [8] C. Tangsadthakun, S. Kanokpanont, N. Sanchavanakit, T. Banaprasert, S. Damrongsakkul,
495 Properties of collagen/chitosan scaffolds for skin tissue engineering, *Journal of Metals,*
496 *Materials and Minerals*. 16, 2006, 37−44.
497 [9] C. V. M. Rodrigues, P. Serricella, A. B. R. Linhares, R. M. Guerdes, R. Borojevic, M. A.
498 Rossi, M. E. L. Duarte, M. Farin, Characterization of a bovine collagen–hydroxyapatite
499 composite scaffold for bone tissue engineering, *Biomaterials*. **24**, 2003, 4987−4997.
500 [10] P. Clark, The effects of topographic and mechanical properties of materials on cell
501 behavior, *Critical Reviews in Biocompatibility*. **5**, 1990, 343−362.
502 [11] M. Y. Yan, B. F. Li, X. Zha, S. Qin, Effect of concentration, pH and ionic strength on the
503 kinetic self-assembly of acid-soluble collagen from walleye pollock (Theragra chalcogramma)
504 skin, *Food Hydrocoll*. **29**, 2012, 199−204.
505 [12] W. J. Landis, R. Jacquet, Association of calcium and phosphate ions with collagen in the
506 mineralization of vertebrate tissues, *Calcif Tissue Int*. **93**, 2013, 329−337.
507 [13] J. R. Harrisa, A. Soliakovc, R. J. Lewisa, In vitro fibrillogenesis of collagen type I in
508 varying ionic and pH conditions, *Micron*. **49**, 2013, 60−68.

509 [14] G. C. Wood, The formation of fibrils from collagen solutions, *J. Biochem*. **75**, 1960,
510 605−612.
511 [15] T. Hayashi, Y. Nagai, Factors affecting the interactions of collagen molecules as observed
512 by *in vitro* fibril formation II. Effects of species and concentrations of anions, *J. Biochem*. **72**,
513 1972, 749−758.
514 [16] Y. P. Li, A. Asadi, M. R. Monroe, E. P. Douglas, pH effects on collagen fibrillogenesis *in*
515 *vitro*: Electrostatic interactions and phosphate binding, *Mater. Sci. Eng. C-Mater. Biol. Appl*.
516 **29**, 2009, 1643−1649.
517 [17] V. Gauba, J. D. Hartgerink, Self-assembled heterotrimeric collagen triple helices directed
518 through electrostatic interactions, *J. Am. Chem. Soc.* **129**, 2007, 2683−2690.
519 [18] E. L. Mertz, S. Leikin, Interactions of inorganic phosphate and sulfate anions with
520 collagen, *Biochemistry*. **43**, 2004, 14901−14912.
521 [19] R. Parenteau-Bareil, R. Gauvin, F. Berthod, Collagen-based biomaterials for tissue
522 engineering applications, *Materials*. **3**, 2010, 1863−1887.
523 [20] R. Duan, J. J. Zhang, X. Q. Du, X. C. Yao, K. Konno, Properties of collagen from skin,
524 scale and bone of carp (*Cyprinus carpio*), *Food Chem*. **112**, 2009 702−706.
525 [21] J. J. Zhang, R. Duan, C. Ye, K. Konno, Isolation and characterization of collagens from
526 scale of silver carp (*hypophthalmichthys molitrix*), *J. Food. Biochem*. **34**, 2010, 1343−1354.

527 [22] J. M. Sanchez-Vizcaino, L. Mur, J. C. Gomez-Villamandos, L. Carrasco, An update on
528 the epidemiology and pathology of African swine fever, *J. Comp. Path*. **152**, 2015, 9−21.
529 [23] E. Wombwell, M. T. Fangman, A. K. Yoder, D. L. Spero, Religious barriers to measles
530 vaccination, *J Community Health*. **40**, 2015, 597−604.
531 [24] P. Kittiphattanabawon, S. Benjakul, W. Visessanguan, T. Nagai, M Tanaka,
532 Characterisation of acid-soluble collagen from skin and bone of bigeye snapper (*Priacanthus*
533 *tayenus*), *Food Chem*. **89**, 2005, 363−372.
534 [25] T. Nagai, N. Suzuki, Isolation of collagen from fish waste material - skin, bone and fins,
535 *Food Chem*. **68,** 2000, 277−281.
536 [26] S. Yunoki, N. Nagai, T. Suzuki, M. Munekata, Novel biomaterial from reinforced salmon
537 collagen gel prepared by fibril formation and cross-linking, *J. Biosci. Bioeng*. **98,** 2004,
538 40−47.
539 [27] X. Zhang, M. Ookawa, Y. K Tan, K. Ura, S. Adachi, Y. Takagi, Biochemical
540 characterisation and assessment of fibril-forming ability of collagens extracted from Bester
541 sturgeon *Huso huso* × *Acipenser ruthenus*, *Food Chem*. **160**, 2014, 305−312.
542 [28] G. Pogany, D. J. Hernandez, K. G. Vogel, The *in vitro* interaction of proteoglycans with
543 type I collagen is modulated by phosphate, *Arch Biochem Biophys*. 313, 1994, 102−111.

544 [29] D. W. Meng, H. Tanaka, T. Kobayashi, H. Hatayama, X. Zhang, K. Ura, S. Yunoki, Y.
545 Takagi, The effect of alkaline pretreatment on the biochemical characteristics and
546 fibril-forming abilities of types I and II collagen extracted from bester sturgeon by-products,
547 *Int. J. Biol. Macromol.* **131**, 2019, 572−580.
548 [30] O. H. Lowry, N. J. Rosebrough, A. L. Farr, R. J. Randall, Protein measurement with the
549 folin phenol reagent, *J. Biol. Chem.* **193,** 1951, 265−275.
550 [31] Y. Nomura, S. Toki, Y. Ishii, K. Shirai, The physicochemical property of shark type I
551 collagen gel and membrane, *J. Agric. Food Chem*. **48**, 2000, 2028−2032.
552 [32] I. Bae, K. Osatomi, A. Yoshida, A. Yamaguchi, K. Tachibana, T. Oda, K. Hara,
553 Characteristics of a self-assembled fibrillar gel prepared from red stingray collagen, *Fish Sci*.
554 **75**, 2009, 765−770.
555 [33] Y. J. Zhang, P. S. Cremer, Interactions between macromolecules and ions: the Hofmeister
556 series, *Curr. Opin. Chem. Biol*. **10**, 2006, 658−663.
557 [34] Y. P. Li, E. P. Douglas, Effects of various salts on structural polymorphism of
558 reconstituted type I collagen fibrils, *Colloids Surf. B Biointerfaces*. **112**, 2013, 42−50.
559 [35] D. A. Cisneros, C. Hung, C. M. Franz, D. J. Muller, Observing growth steps of collagen
560 self-assembly by time-lapse high-resolution atomic force microscopy, *J. Struct. Biol*. **154**,
561 2006, 232−245.

562 [36] R. A. Gelman, D. C. Poppke, K. A. Piez, Collagen fibril formation *in Vitro*, *J. Biol. Chem*.
563 **254**, 1979, 11741−11745.
564 [37] R. L. Trelatad, V. M. Catanese, D. F. Rubin, Collagen fibrillogenesis: Intermediate
565 aggregates and order. *Proc. Matl. Acad. Sci.* USA 73, 4027.
566 [38] D. L. Christiansen, E. K. Huang, F. H. Silver, Assembly of type I collagen: fusion of
567 fibril subunits and the influence of fibril diameter on mechanical properties. *Matrix Biol.* **19**,
568 2000, 409−420.
569 [39] F. H. Silver, R. L. Trelstad, Linear aggregation and the turhidimetric lag Phase: Type I
570 Collagen Fibrillogenesis *in vitro*, *J. Theor. Biol*. **81**, 1979, 515−526.
571 [40] J. L. Zhu, L. J. Kaufman, Collagen I self-assembly: revealing the developing structures
572 that generate turbidity, *Biophys. J*. **106**, 2014, 1822−1831.
573 [41] B. R. Williams, R. A. Gelman, D. C. Poppke, K. A. Piez, Collagen Fibril formation.
574 Optimal *in vitro* conditions and preliminary kinetic results, *J. Biol. Chem*. **253**, 1978,
575 6578−6585.
576 [42] M. Saito, Y. Takenouchi, N. Kunisaki, S. Kimura, Complete primary structure of rainbow
577 trout type I collagen consisting of α1(I)α2(I)α3(I) heterotrimers, *Eur. J. Biochem*. **268**, 2001,
578 2817−2827.

579 [43] X. Zhang, Studies on the properties of sturgeon collagen as potential biomaterials, Ph. D.
580 Thesis, Hokkaido University, 2015, pp 123.
581 [44] J. L. Bailey, P. J. Critser, C. Whittington, J. L. Kuske, M. C. Yoder, S. L. Voytik-Harbin,
582 Collagen oligomers modulate physical and biological properties of three-dimensional
583 self-assembled matrices, *Biopolymers*. **95**, 2011, 77−93.
584 [45] G. Mosser, A. Anglo, C. Helary, Y. Bouligand, M. M. Giraud-Guille, Dense tissue-like
585 collagen matrices formed in cell-free conditions, *Matrix Biol*. **25**, 2006, 3−13.
586 [46] X. Zhang, S. Adachi, K. Ura, Y. Takagi, Properties of collagen extracted from Amur
587 sturgeon *Acipenser schrenckii* and assessment of collagen fibrils *in vitro*, *Int. J. Biol.*
588 *Macromol*. **137**, 2019, 809−820.
589 [47] C. N. Grover, J. H. Gwynne, N. Pugh, S. Hamaia, R. W. Farndale, S. M. Best, R. E.
590 Cameron, Crosslinking and composition influence the surface properties, mechanical
591 stiffness and cell reactivity of collagen-based films, *Acta Biomater.* **8**, 2012, 3080−3090.
592 [48] Y. Liu, Y. Ji, K. Ghosh, R. A. F. Clark, L. Huang, M. H. Rafailovich, Effects of fiber
593 orientation and diameter on the behavior of human dermal fibroblasts on electrospun PMMA
594 scaffolds, *J. Biomed. Mater. Res*. **90**, 2009, 1092−1106.
595 [49] J. Friedrichs, A. Taubenberger, C. M. Franz, D. J. Muller, Cellular remodelling of
596 individual collagen fibrils visualized by time-lapse AFM, *J. Mol. Biol*. **372**, 2007, 594−607.

[50] R. K Assoian, M. A. Schwartz, Coordinate signaling by integrins and receptor tyrosine kinases in the regulation of G1 phase cell-cycle progression, *Curr. Opin. Genet. Dev*. **11**, 2001, 48−53.

[51] J. W. Xie, X. R. Li, J. Lipner, C. N. Manning, A. G. Schwartz, S. Thomopoulos, Y. N. Xia, Aligned-to-random nanofiber scaffolds for mimicking the structure of the tendon-to-bone insertion site, *Nanoscale*. **2**, 2010, 923−926.

[52] S. A. Tsakonas, M. D. Rand, R. J. Lake, Notch signaling: cell fate control and signal integration in development, *Science*. **284**, 1999, 770−777.

[53] S. Moroi, T. Miura, T. Tamura, X. Zhang, K. Ura, Y. Takagi, Self-assembled collagen fibrils from the swim bladder of Bester sturgeon enable alignment of MC3T3-E1 cells and enhance osteogenic differentiation, *Mater. Sci. Eng., C*. **104**, 2019, 109925.

608 **Figure captions**

609 **Fig. 1.** Effects of phosphate ion concentration on *in-vitro* formation of fibrils of (A) swim

610 bladder and (B) skin collagens of Bester sturgeon.

611

612 **Fig. 2.** Effects of phosphate ion concentration on the degree of fibril formation of (A) swim

613 bladder and (B) skin collagens of Bester sturgeon. Columns and bars represent mean and

614 standard error for three experiments. Differences between groups with different letters are

615 significant (Tukey–Kramer post-hoc test, $p < 0.01$).

616

617 **Fig. 3.** Scanning electron micrographs of swim bladder and skin fibrils formed at 21 °C for 1

618 h. Scale bars: 5 μm. Black and white arrows indicate fusiform and bundle structures in SBC

619 and SC, respectively.

620

621 **Fig. 4.** Diameter distributions of swim bladder and skin collagen fibrils formed at 21 °C for 1

622 h.

623

624 **Fig. 5.** DSC curves of (A) swim bladder and (A) skin collagen fibrils formed at 21 °C for 1 h.

625 Black arrowheads indicate maximum transition temperatures.

626

627 **Fig. 6.** Scanning electron micrographs of bottom surfaces of cell culture wells coated with
628 swim bladder and skin collagen fibrils. Scale bars: 5 μm. Black arrows indicate fusiform
629 structures in SBC-coated wells.

630

631 **Fig. 7.** Phase-contrast microscopy images of L929 cells cultured for 6 and 24 h. Scale bars: 75
632 μm.

633

634 **Fig. 8.** Scanning electron micrograph images of L929 cells cultured for 2 days. White arrows
635 show the direction of collagen fibril alignment. Scale bars: 10 μm.

636

637 **Fig. 9.** Proliferation of L929 cells cultured for 5 days. Columns and bars represent mean and
638 standard error for six measurements. Differences between groups with different letters are
639 significant (Tukey–Kramer post-hoc test, $p < 0.01$).

Fig.1

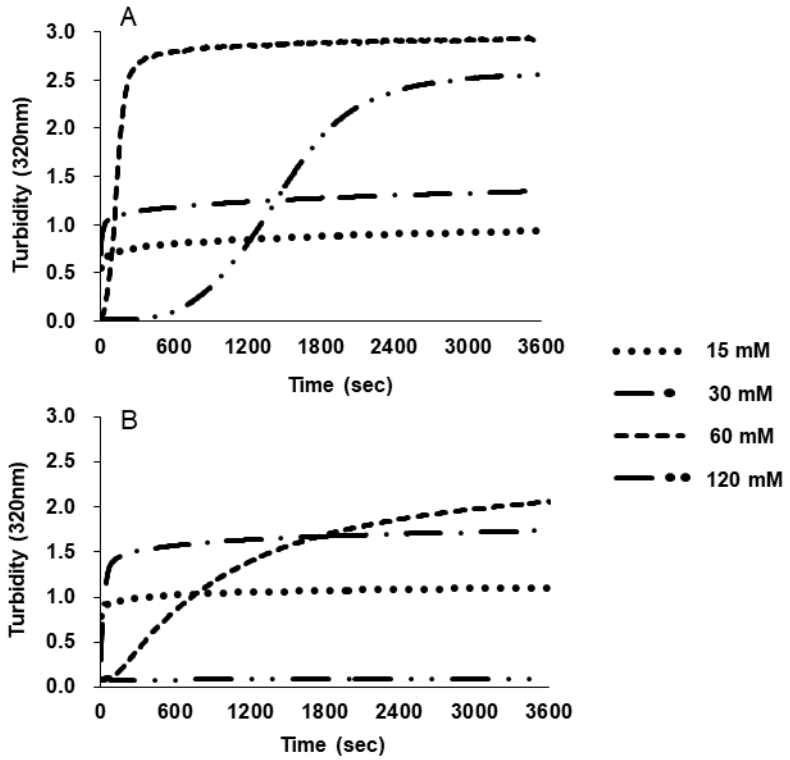

A
B
Turbidity (320nm)
Time (sec)
0.0
0.5
1.0
1.5
2.0
2.5
3.0
0
600
1200
1800
2400
3000
3600
15 mM
30 mM
60 mM
120 mM

Fig.2

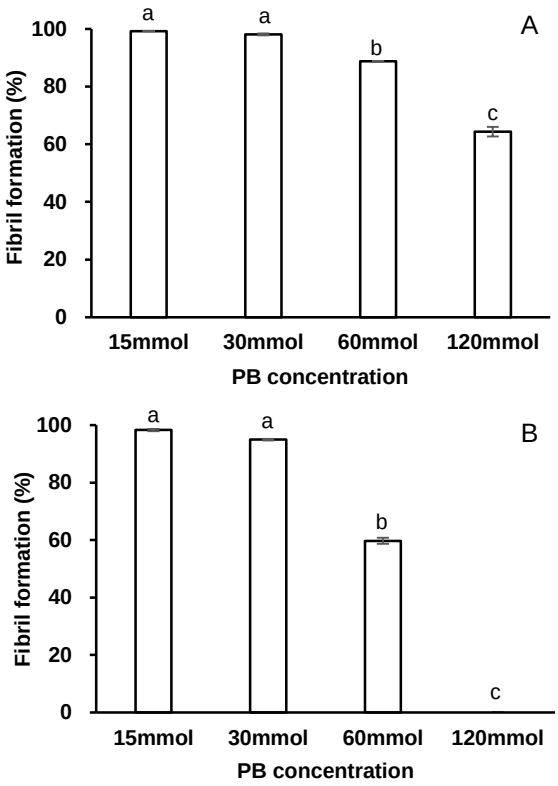

A
Fibril formation (%)
100
80
60
40
20
0
a
a
b
c
15mmol
30mmol
60mmol
120mmol
PB concentration
B
Fibril formation (%)
100
80
60
40
20
0
a
a
b
c
15mmol
30mmol
60mmol
120mmol
PB concentration

Fig.3

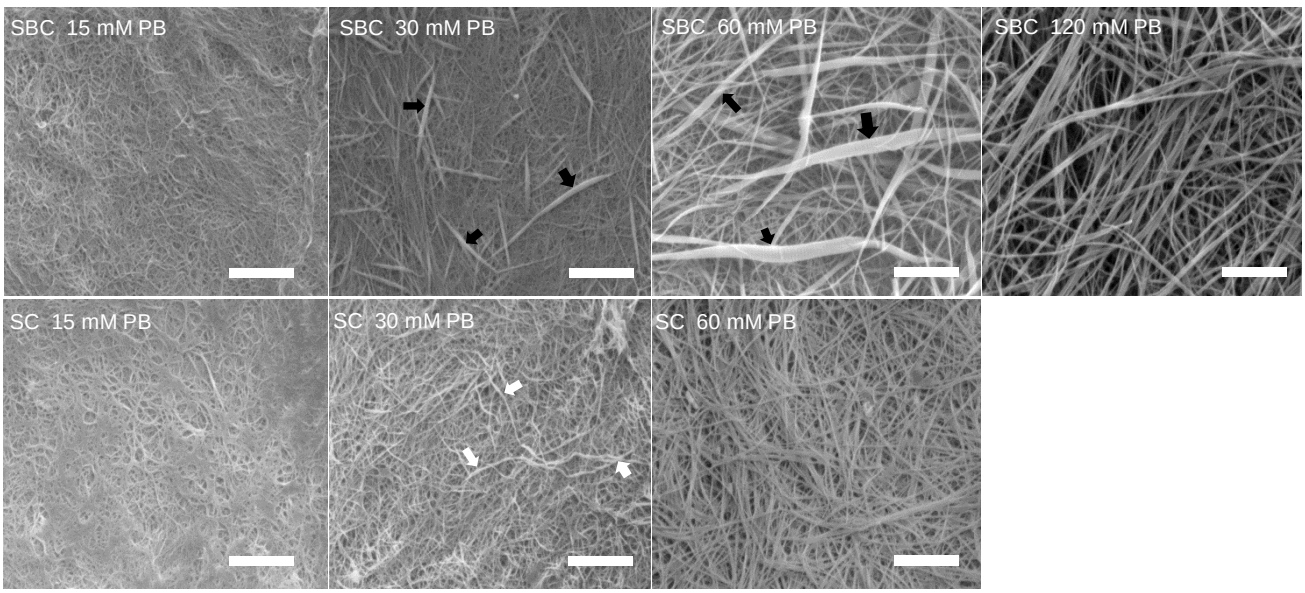

SBC 15 mM PB
SBC 30 mM PB
SBC 60 mM PB
SBC 120 mM PB
SC 15 mM PB
SC 30 mM PB
SC 60 mM PB

Fig.4

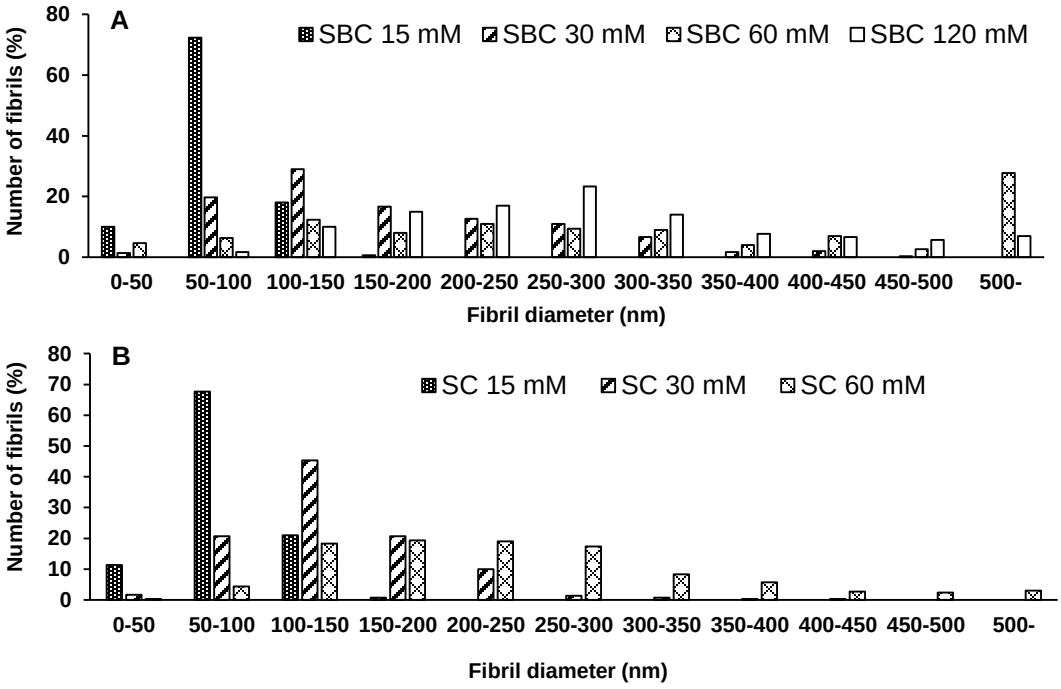

A
SBC 15 mM
SBC 30 mM
SBC 60 mM
SBC 120 mM
Number of fibrils (%)
80
60
40
20
0
0-50
50-100
100-150
150-200
200-250
250-300
300-350
350-400
400-450
450-500
500-
Fibril diameter (nm)
B
SC 15 mM
SC 30 mM
SC 60 mM
Number of fibrils (%)
80
70
60
50
40
30
20
10
0
0-50
50-100
100-150
150-200
200-250
250-300
300-350
350-400
400-450
450-500
500-
Fibril diameter (nm)

Fig.5

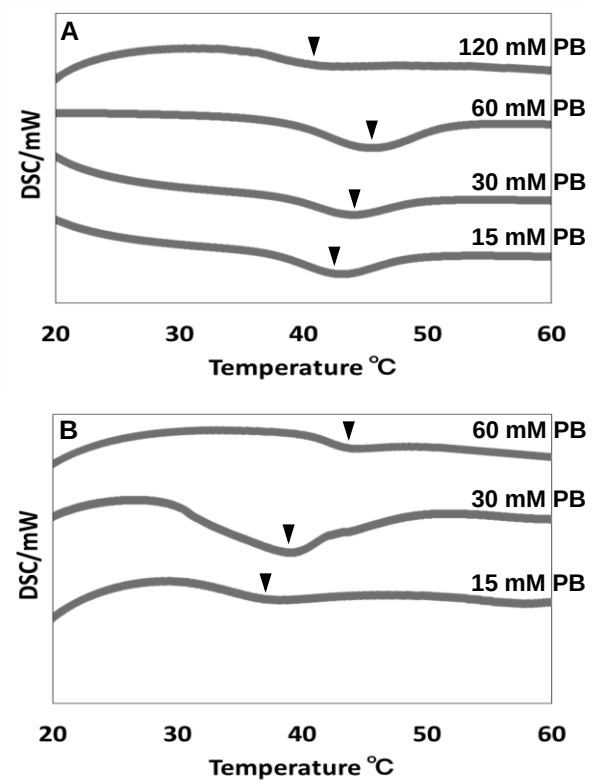

A
120 mM PB
60 mM PB
30 mM PB
15 mM PB
DSC/mW
20
30
40
50
60
Temperature ℃
B
60 mM PB
30 mM PB
15 mM PB
DSC/mW
20
30
40
50
60
Temperature ℃

Fig.6

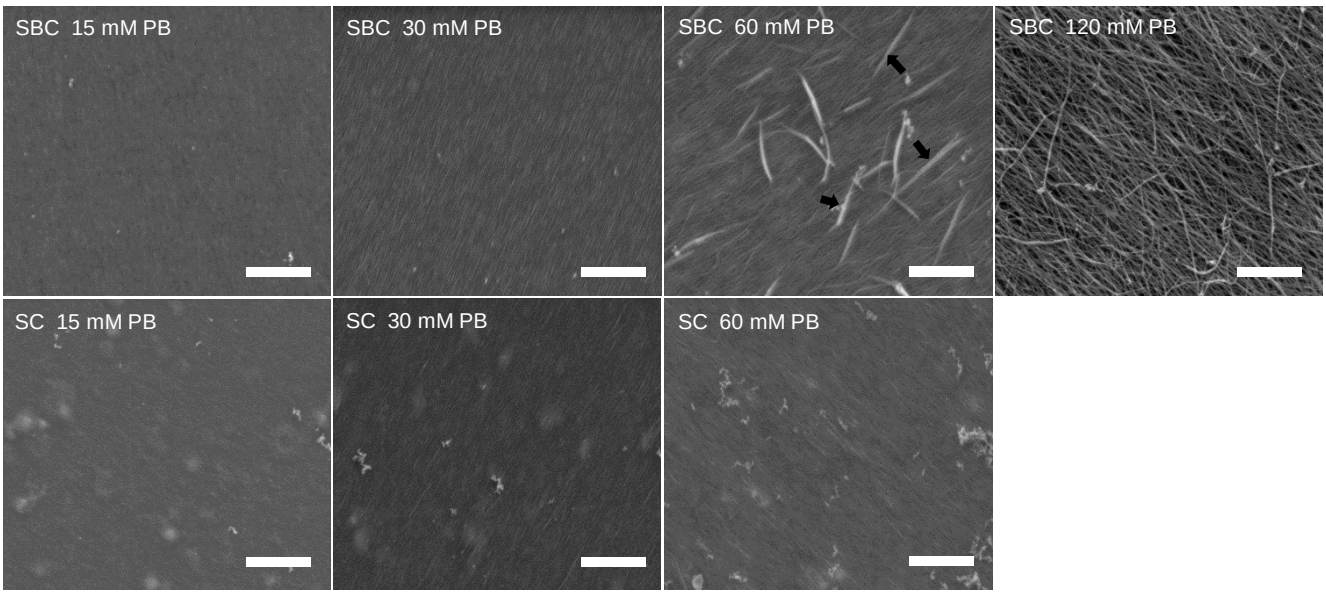

SBC 15 mM PB
SBC 30 mM PB
SBC 60 mM PB
SBC 120 mM PB
SC 15 mM PB
SC 30 mM PB
SC 60 mM PB

Fig.7

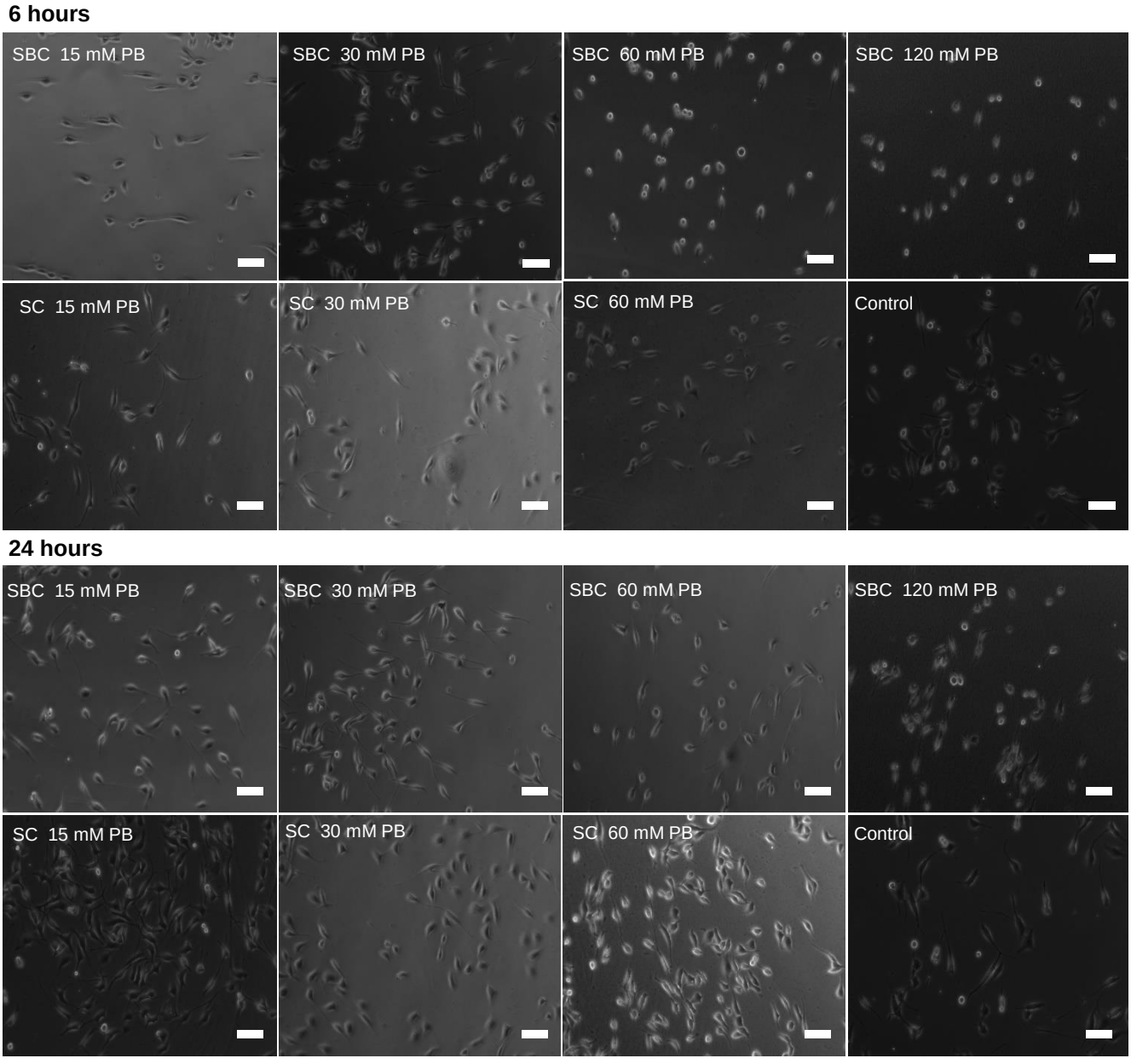

6 hours
SBC 15 mM PB
SBC 30 mM PB
SBC 60 mM PB
SBC 120 mM PB
SC 15 mM PB
SC 30 mM PB
SC 60 mM PB
Control
24 hours
SBC 15 mM PB
SBC 30 mM PB
SBC 60 mM PB
SBC 120 mM PB
SC 15 mM PB
SC 30 mM PB
SC 60 mM PB
Control

Fig.8

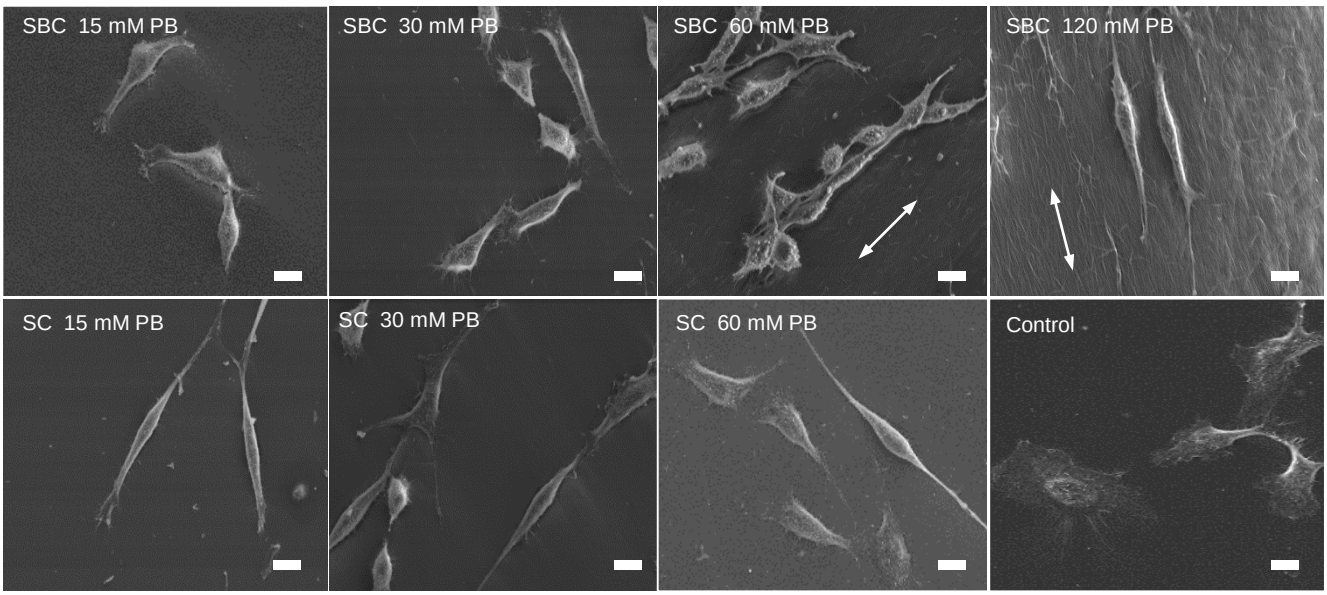
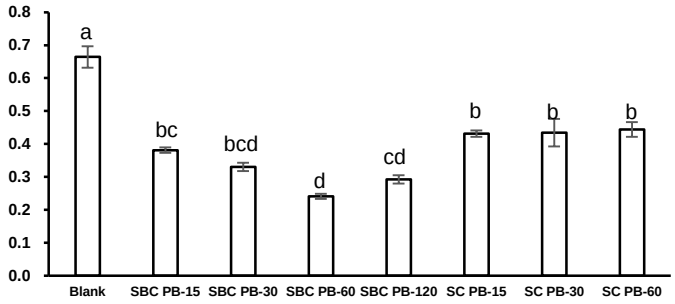

SBC 15 mM PB
SBC 30 mM PB
SBC 60 mM PB
SBC 120 mM PB
SC 15 mM PB
SC 30 mM PB
SC 60 mM PB
Control

Fig.9


0.8
0.7
0.6
0.5
0.4
0.3
0.2
0.1
0.0
a
bc
bcd
d
cd
b
b
b
Blank
SBC PB-15
SBC PB-30
SBC PB-60
SBC PB-120
SC PB-15
SC PB-30
SC PB-60